Front. Phys. 12(5), 121101 (2017)
DOI 10.1007/s11467-016-0615-0

Research article

Pair production in strong $SU(2)$ background fields

Mo-Ran Jia[1], **Zi-Liang Li**[1], **Chong Lv**[1], **Feng Wan**[1], **Bai-Song Xie**[1,2,†]

[1] *College of Nuclear Science and Technology, Beijing Normal University, Beijing 100875, China*
[2] *Beijing Radiation Center, Beijing 100875, China*
Corresponding author. E-mail: † *bsxie@bnu.edu.cn*
Received May 26, 2016; accepted July 14, 2016

Fermion particle pair production in strong $SU(2)$-gauge chromoelectric fields is studied using the Boltzmann–Vlasov equation in a classical way. The existence of a preproduction process in a classical description is shown using the distribution evolution of non-Abelian particle production. It is interesting to find that the distribution of the particle number density is centered on two islands and shows a split on the color charge sphere as it evolves, ultimately reaching a steady state that is related to the amplitude and variation of the field.

Keywords pair production, $SU(2)$-gauge chromoelectric field, classical and semiclassical technique, Boltzmann–Vlasov equation

PACS numbers 11.15.-q, 12.38.-t, 52.65.Ff

1 Introduction

Experiments on high-energy collisions of heavy ions, which are thought to produce a quark–gluon plasma, are conducted in both the Relativistic Heavy Ion Collider and Large Hadron Collider. Modeling this plasma using full quantum field theory has been proven particularly difficult. Because it is hard to deal with particles of different colors for different flavors under gauge invariance and renormalization, an appropriate approximation theory is urgently needed. Thus, a series of works has been conducted using effective classical theories [1–8], as summarized in Ref. [9], and has been expanded to problems of particle production.

For the problem of particle production, Schwinger developed a proper time method to calculate the particle production via a tunneling mechanism in quantum electrodynamics (QED) theory [10]. For the QED case, Dawson *et al.* studied particle production using a semiclassical approach based on the Boltzmann–Vlasov (B–V) transport equation with an instantaneous source term [11, 12] and compared the B–V results with numerical simulations of the full quantum treatment. We have also studied the relevant pair production problem in the QED case, e.g., [13–16]. In addition, we recently studied the nonperturbative signatures in particle momentum spectra of pair production by solving the quantum Vlasov equation or using the Dirac–Heisenberg–Wigner formalism, especially for general elliptically polarized fields [17–19]. On the other hand, naturally, the problem of particle production is expected to be expanded to the quantum chromodynamics case. For example, soft gluon production [20] and quark–antiquark production [21] in a constant chromoelectric background field were studied by Nayak and his coauthor. Recently, Dawson *et al.* studied this problem including the backreaction effects [22]. They have also studied the Casimir dependence of the transverse distribution in non-Abelian particle production [23]. Similar work in the $SU(2)$ case has also been performed by Skokov and Levái using the Wigner function formalism [24].

It is also necessary and meaningful to study the process of non-Abelian particle production. Using the B–V equation as an approximate theory will simplify the calculation and also give a clear physical picture. Further, in our paper, Wong's equations in Ref. [25] are used as the equations of motion. Because non-Abelian particle production is related to the Casimir invariants, we will give the distribution of particle production on the color charge sphere in the $SU(2)$ case. Further, we will discuss the evolution of the distribution in different background fields. Finally, we will give the total number of particles produced.

For simplicity, we treat the particles as point particles with classical color, and we ignore the backreaction effect because it is an order lower than that of the background field [22] assuming the low density approximation. Note that in realistic situations, the collision effect should be taken into account. However, in our classical calculation using a simple or/and insufficiently realistic model, the preproduction process we found, which is our main point, still exhibits some interesting features. It is helpful to deepen the understanding of the relevant problem. On the other hand, we will also use the Schwinger source when introducing different fields, as in Ref. [26], because the field can be regarded as varying sufficiently slowly.

The paper is organized as follows. In Section 2, we introduce Wong's equation in semiclassical transport theory. In Section 3, we define the distribution function with the measures in phase space. In Section 4, we derive the B–V equation and introduce a classical source term. In Section 5, we give the numerical methods and numerical results for a special case. Further, in the final section, we summarize our numerical results and present our conclusions. In the Appendix, we give some derivation of Wong's equations and the solution of the B–V equation using the method of characteristics.

2 Wong's equations in semiclassical theory

A theory describing the Yang–Mills (YM) field and isotopic-spin-carrying particles in the classical limit was derived by Wong in Ref. [25]. Within a microscopic description, the trajectories in space are known exactly and read as

$$m\frac{\mathrm{d}\hat{x}^\mu}{\mathrm{d}t} = \hat{p^\mu}, \tag{1}$$

$$m\frac{\mathrm{d}\hat{p^\mu}}{\mathrm{d}t} = g\hat{Q}^a F_a^{\mu\nu}(\hat{x})\hat{p}_\nu, \tag{2}$$

$$m\frac{\mathrm{d}\hat{Q}^a}{\mathrm{d}t} = gf^{abc}A_\mu^b(\hat{x})\hat{Q}^c\hat{p}^\mu, \tag{3}$$

where

$$F^{a,\mu\nu}(x) = \partial^\mu A^{a,\nu}(x) - \partial^\nu A^{a,\mu}(x) + gf^{abc}A^{b,\mu}(x)A^{c,\nu}(x) \tag{4}$$

is a general YM field and satisfies

$$D_\mu^{a,c}(x)F^{c,\mu\nu}(x) = \langle J^{a,\nu}(x)\rangle. \tag{5}$$

After some approximation and introduction of the proper time τ for particles, the equations read

$$m\frac{\mathrm{d}x^\mu}{\mathrm{d}\tau} = p^\mu, \tag{6}$$

$$m\frac{\mathrm{d}p^\mu}{\mathrm{d}\tau} = gQ^a F_a^{\mu\nu}p_\nu, \tag{7}$$

$$m\frac{\mathrm{d}Q^a}{\mathrm{d}\tau} = gf^{abc}A_\mu^b Q^c p^\mu. \tag{8}$$

The equations are obtained by the substitutions $\hat{x^\mu} \to x^\mu, \hat{p^\mu} \to p^\mu, \hat{Q}^a \to Q^a$, and will be used as the leading order of motion for point particles in soft gauge fields.

3 Microscopic distribution function

To describe the ensemble of particles in phase space, it is convenient to define a distribution function, which depends on the entire set of coordinates, $\boldsymbol{x}, \boldsymbol{p}, \boldsymbol{Q}$. Here, we introduce the one-particle distribution functions $f(\boldsymbol{x}, \boldsymbol{p}, \boldsymbol{Q})$ and $n(\boldsymbol{x}, \boldsymbol{p}, \boldsymbol{Q})$; then the color current density energy-momentum tensor and particle number density are given by

$$t^{\mu\nu}(\boldsymbol{x}) = \int \mathrm{d}\boldsymbol{P}\mathrm{d}\boldsymbol{Q}p^\mu p^\nu f(\boldsymbol{x}, \boldsymbol{p}, \boldsymbol{Q}), \tag{9}$$

$$j_a^\mu(\boldsymbol{x}) = \int \mathrm{d}\boldsymbol{P}\mathrm{d}\boldsymbol{Q}p^\mu Q_a f(\boldsymbol{x}, \boldsymbol{p}, \boldsymbol{Q}), \tag{10}$$

$$n(\boldsymbol{x}) = \int \mathrm{d}\boldsymbol{P}\mathrm{d}\boldsymbol{Q} f(\boldsymbol{x}, \boldsymbol{p}, \boldsymbol{Q}), \tag{11}$$

where

$$\mathrm{d}\boldsymbol{P} = \mathrm{d}^4 p\theta(p_0)\delta(p^2 - m^2), \tag{12}$$

$$\mathrm{d}\boldsymbol{Q} = \mathrm{d}^3 Q c_R \delta(Q_a Q^a - q_2) \tag{13}$$

are the momentum measure and $SU(2)$ group measure, respectively, which constrain the mass-on-shell condition, positive energy, and conservation of the group Casimirs. Further, c_R and q_2 are parameters related to particles and their representations. Here, unlike the case in Ref. [1], we just define one distribution function for both particles and antiparticles in the $SU(2)$ gauge, which are distinguished by the color charge $\boldsymbol{Q}$. From Wong's equations in the $SU(2)$ case, we can write $\boldsymbol{Q}$ in spherical coordinates as

$$Q_1 = J\sin\theta\cos\phi, \tag{14}$$

$$Q_2 = J\sin\theta\sin\phi, \tag{15}$$

$$Q_3 = J\cos\theta, \tag{16}$$

and we can find that $c_R = 2/(\sqrt{3}\pi)$, $q_2 = 3/4$, and $J = \sqrt{3}/2$ in Refs. [9, 22].

4 Boltzmann–Vlasov equation with a classical source term

4.1 Boltzmann–Vlasov equation

The B–V equation can be derived by considering the total derivative of the distribution function $f(\boldsymbol{x}, \boldsymbol{p}, \boldsymbol{Q})$. Considering the proper time τ, we have

$$m\frac{\mathrm{d}f(\boldsymbol{x}, \boldsymbol{p}, \boldsymbol{Q})}{\mathrm{d}\tau} = p^\mu \mathcal{B}_\mu[\boldsymbol{A}](\tau)f(\boldsymbol{x}, \boldsymbol{p}, \boldsymbol{Q}), \tag{17}$$

where $\mathcal{B}_\mu[\boldsymbol{A}](\tau) = \mathcal{D}_\mu[\boldsymbol{A}] - g\boldsymbol{Q}\cdot\boldsymbol{F}_{\mu\nu}(\tau)\partial_{p_\nu}$ is the B–V differential operator, and $\mathcal{D}_\mu[\boldsymbol{A}] = \partial_\mu - g\boldsymbol{A}(\tau)\cdot\boldsymbol{Q}\times\partial_{\boldsymbol{Q}}$ is a color-covariant derivative operator. Thus, if we require that p be on-shell and $\boldsymbol{Q}$ satisfy the Casimir relation, the B–V equation is given by

$$p_\mu \mathcal{B}[\boldsymbol{A}](\tau) f(\boldsymbol{x},\boldsymbol{p},\boldsymbol{Q}) = p^t \boldsymbol{C}(\boldsymbol{x},\boldsymbol{p},\boldsymbol{Q}). \tag{18}$$

Here we ignore collision effects, and $C(\boldsymbol{x},\boldsymbol{p},\boldsymbol{Q})$ is a source term. Inserting Eqs. (6)–(8) into Eq. (17), the B–V equation becomes

$$\left(p^\mu \frac{\partial}{\partial x^\mu} + gQ^a F_a^{\mu\nu} p_\nu \frac{\partial}{\partial p^\mu} + f_{abc} A_\mu^b Q^c \frac{\partial}{\partial Q_a}\right) f(\boldsymbol{x},\boldsymbol{p},\boldsymbol{Q}) = p^t \boldsymbol{C}(\boldsymbol{x},\boldsymbol{p},\boldsymbol{Q}). \tag{19}$$

4.2 Particle production

By using the one-loop approximation of quantum field theory, the particle production rate for fermions [20] is

$$\frac{\mathrm{d}N_{q,\bar{q}}}{\mathrm{d}t\mathrm{d}^3x\mathrm{d}^2p_T} = -\frac{1}{4\pi^3}\sum_{j=1}^{3}|g\lambda_j| \ln[1-\exp(-\pi(p_T^2+m^2)/|g\lambda_j|)], \tag{20}$$

where m is the mass of the quark, and λ_1, λ_2, and λ_3 are the gauge-invariant eigenvalues. All these calculations are based on the Schwinger tunneling effect in a constant chromoelectric field.

For classical particle production, we can make the replacement $E^a(t)T^a \to \boldsymbol{E}(t)\cdot\boldsymbol{Q}$ and replace the sum by integration of $\boldsymbol{Q}$, as in Ref. [22]. For a chromoelectric field that varies slowly, we can also obtain a $\boldsymbol{Q}$-dependent particle production rate $\boldsymbol{C}(\boldsymbol{x},\boldsymbol{p},\boldsymbol{Q})$, which is given by

$$\boldsymbol{C}(\boldsymbol{x},\boldsymbol{p},\boldsymbol{Q}) = |\boldsymbol{Q}\cdot\boldsymbol{E}(\boldsymbol{x})|\boldsymbol{R}(\boldsymbol{x},\boldsymbol{p},\boldsymbol{Q})\delta(p_z), \tag{21}$$

with

$$\boldsymbol{R}(\boldsymbol{x},\boldsymbol{p},\boldsymbol{Q}) = \boldsymbol{P}(\boldsymbol{x},\boldsymbol{p},\boldsymbol{Q})\boldsymbol{S}(\boldsymbol{x},\boldsymbol{p},\boldsymbol{Q}), \tag{22}$$

where

$$\boldsymbol{P}(\boldsymbol{x},\boldsymbol{p},\boldsymbol{Q}) = 1 - 2f_0(\boldsymbol{x},\boldsymbol{p},\boldsymbol{Q}), \tag{23}$$

and

$$\boldsymbol{S}(\boldsymbol{x},\boldsymbol{p},\boldsymbol{Q}) = 1 - \exp\left(-\frac{\pi(\boldsymbol{p}^2+m^2)}{|g\boldsymbol{Q}\cdot\boldsymbol{E}(\boldsymbol{x})|}\right). \tag{24}$$

Here $f_0(\boldsymbol{x},\boldsymbol{p},\boldsymbol{Q})$ is a special distribution function, which is defined as $f_0(\boldsymbol{x},\boldsymbol{p},\boldsymbol{Q}) \equiv f(\boldsymbol{x},\boldsymbol{p}(p_z=0),\boldsymbol{Q})$. Note that most of the particle production occurs at $p_z = 0$ by Pauli blocking at p_z.

5 Numerical results

In this section, we give the numerical methods and results. To simplify the calculation, we choose the gauge potential $A^{a,\mu}(x)$ in the z direction depending only on t for all $a = 1, 2, 3$, which reads as

$$A^{a,\mu}(t) = (0,0,0,A^a(t)). \tag{25}$$

To calculate the distribution of particle production on the $\boldsymbol{Q}$ sphere, we should solve the trajectory equations numerically for the distribution function. Because no particles are produced at $t = 0$, we set $n(0,0,Q) = 0$. We ignore the Pauli blocking effect in our calculation, set $g = 1$, and use the unit $m = 1$. We consider only the particles created with zero momentum in the z direction; then the initial conditions are given as

$$t(\tau_0) = 0, \quad p^t(\tau_0) = m, \tag{26}$$

$$z(\tau_0) = 0, \quad p^z(\tau_0) = 0. \tag{27}$$

For the non-Abelian gauge vector potential, we set $A = (0,0,0)$ initially. We calculate both the constant and cosine chromoelectric fields after giving their amplitudes, E_{const} and $E_{\cos}$, respectively. We choose appropriate constant fields with equal amplitude, and the frequency of the cosine fields is 0.8 in units of $m = 1$.

We distribute the color charges on a $\boldsymbol{Q}$ sphere and consider that the non-Abelian interaction occurs when $\boldsymbol{Q}$ moves on the sphere according to Wong's equations. We take each degree of θ and ϕ on the $\boldsymbol{Q}$ sphere and calculate the produced particle number density as time advances. We take $\mathrm{d}\tau = 0.0005$ and choose $\tau_0 = 0$ to guarantee that production occurs in the light cone. We also fix $\boldsymbol{Q}$ at each step to guarantee that Wong's equations will not be violated.

After solving the trajectory equations numerically and finding the distribution function, we can integrate out the produced particle number density $n(\boldsymbol{x},\boldsymbol{p},\boldsymbol{Q})$. Further, especially for the $SU(2)$ case, we can distribute the color charges on the $\boldsymbol{Q}$ sphere and use θ and ϕ as two parameters to show the distribution of the produced particle number density in contour maps.

In our calculation, we find that the number density is distributed in two islands on the $\boldsymbol{Q}$ sphere, which we regard as a pair of conjugate particles. Further, the distribution on the islands is centrosymmetric. Then we concentrate on describing the phenomena on one island.

In Fig. 1, the distribution of the number density is initially centered on the island. As time advances, the distribution center splits into two parts, which move to each edge of the island. The distribution becomes steady when the time is sufficiently long. In Fig. 2, we find that the steady state that the distribution can reach is related to the amplitude of the field. In a small-amplitude field, the center will not split at all, but the split occurs when the amplitude become larger. Further, the two parts of the center are distributed closer to the edge as the amplitude of the field increases.

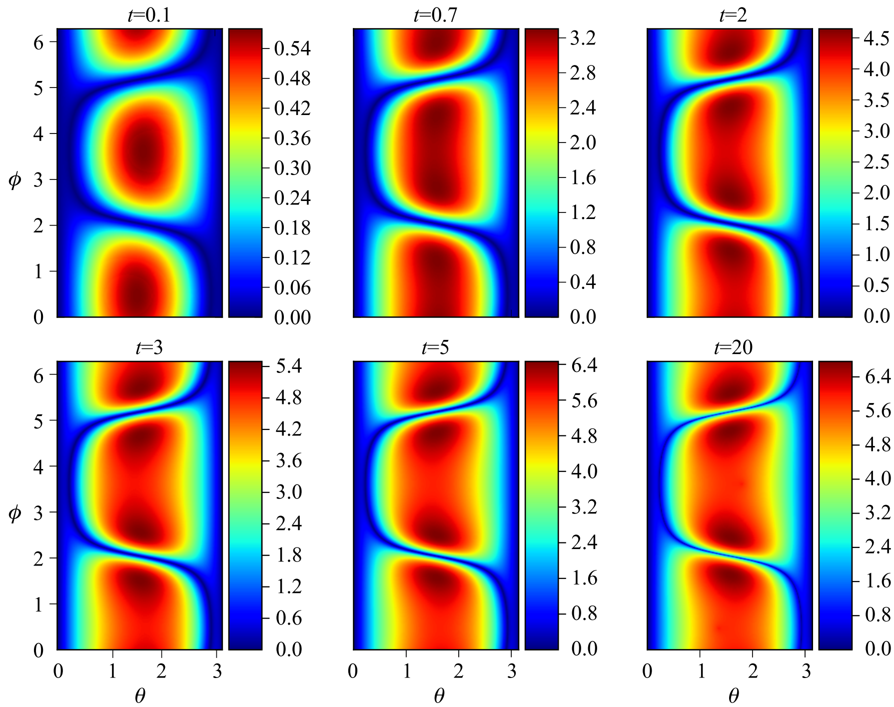

Fig. 1 Contour of produced particle number density on $\boldsymbol{Q}$ sphere in a constant chromoelectric field at different time. The color bar has been multiplied by 10^{-5}.

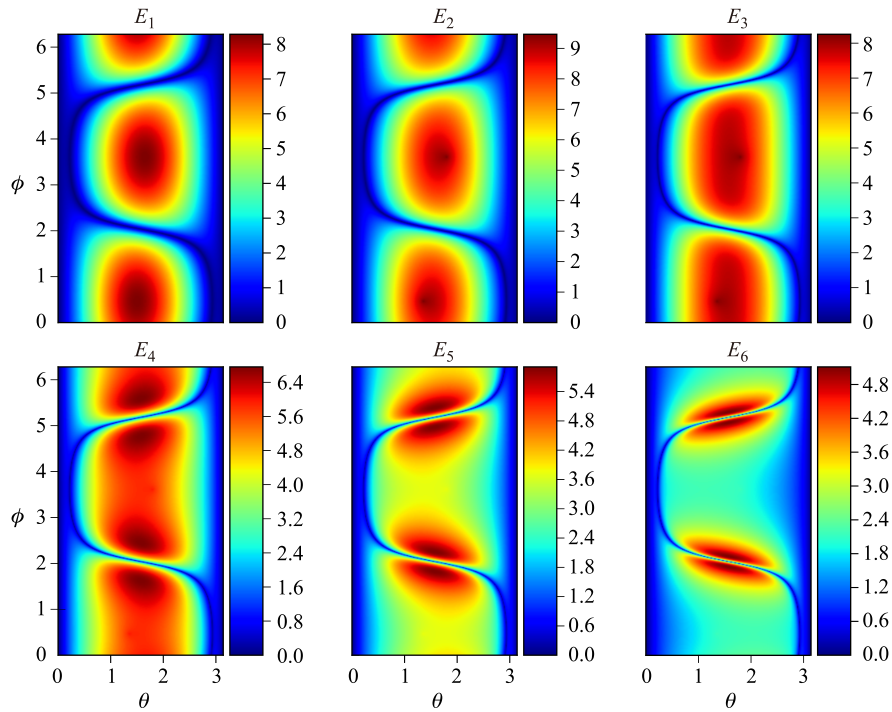

Fig. 2 Contour of produced particle number density on $\boldsymbol{Q}$ sphere in constant chromoelectric fields at $t = 20$ for different field amplitude of $E_1 = (1, 0.5, 0.25)$, $E_2 = (2, 1, 0.5)$, $E_3 = (3, 1.5, 0.75)$, $E_4 = (4, 2, 1)$, $E_5 = (8, 4, 2)$, and $E_6 = (16, 8, 4)$, respectively. The color bar has been multiplied by 10^{-5}.

In Fig. 3, we can also find the same phenomenon in a slowly varying field. The difference is that a fluctuation structure appears in the contour map as time advances. Further, compared to the behavior under the constant field, the two split parts are closer to the edge when they reach the steady state. Figure 4 shows the contour maps in cosine fields of different amplitudes; the results are the same as those for the constant field except that a delicate fluctuation structure exists.

Our calculated temporal evolution lasted until $t = 70$, but we show only the contour maps that describe the splitting process of the distribution center. In our calculated temporal evolution, we also find that the two parts of the split distribution center are close to the edge but never escape from the island. The calculation for fields of different amplitude also shows this confinement behavior. From Figs. 2 and 4, it seems that there is a critical amplitude that leads to splitting of the distribution center. Because it is hard to define the splitting strictly in a classical calculation, we just choose some discrete

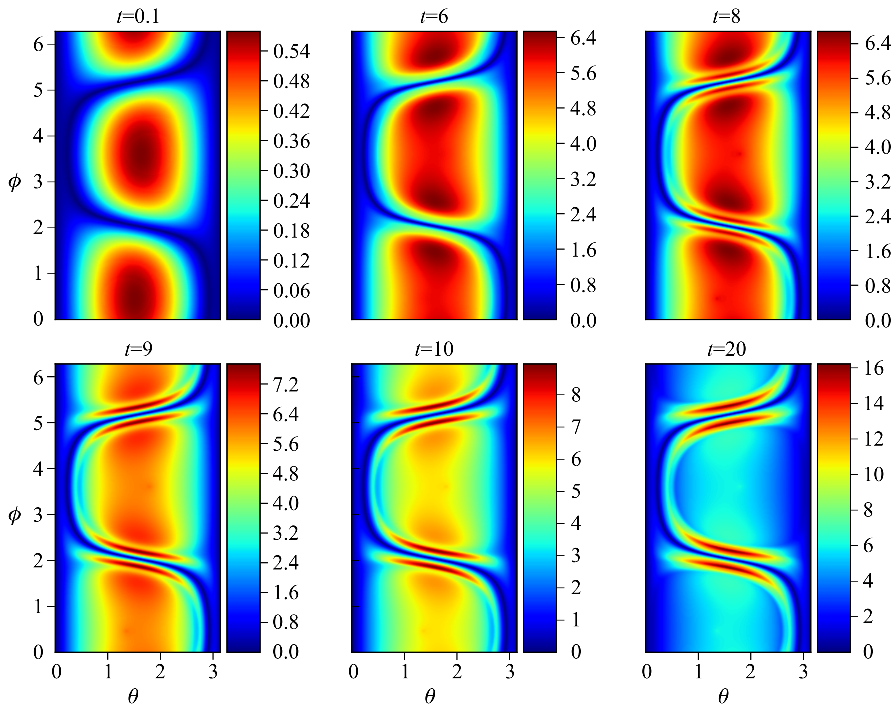

Fig. 3 The same as in Fig. 1 except in a cosine chromoelectric field.

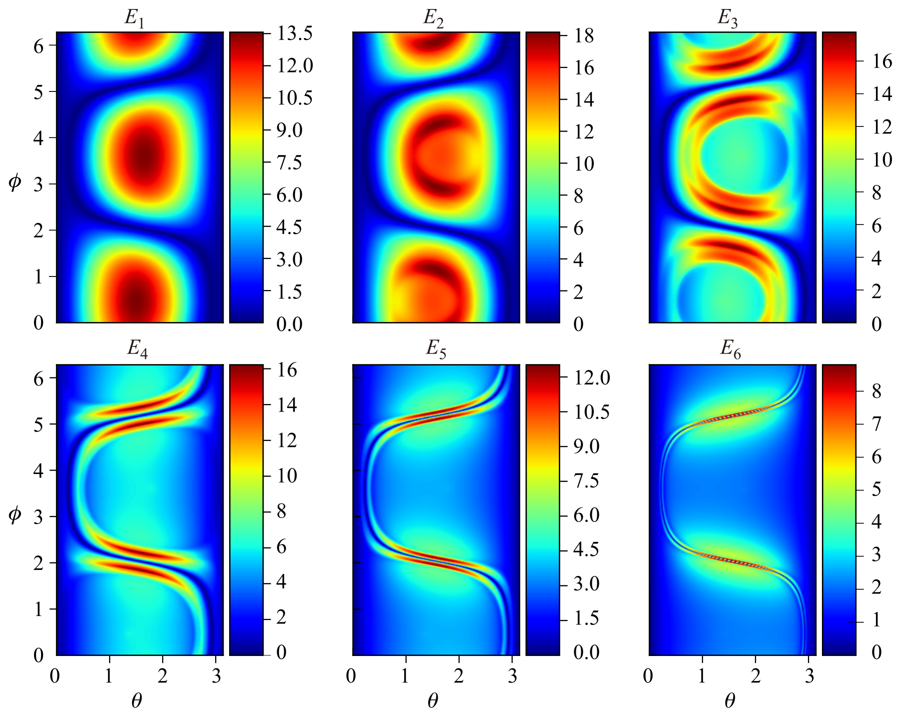

Fig. 4 The same as in Fig. 2 except in a cosine chromoelectric field.

amplitudes.

In Fig. 5, we show the evolution of the total particle number. We find that the total particle number increases more quickly in the constant field than in the cosine field when $t < 8$ but more slowly in the constant field than in the cosine field when $t > 8$. Comparing Fig. 5 with Figs. 1 and 3, we find that in the constant field, the distribution reaches the steady state more quickly, but the total particle number is less than that in the cosine field.

In Fig. 6, we show the total particle number in fields of different amplitude at $t = 20$, which is long enough to form a steady distribution on the $\boldsymbol{Q}$ sphere. We find that the total particle number increases at first but then decreases as the amplitude grows in both the constant and cosine fields. Further, we find that the largest total particle number occurs in field E_2, and the smallest total particle number occurs in field E_6, yet the distribution center splits subtly in field E_2 but obviously in field E_6. We also find that the total particle number in the constant field is less than that in the cosine field when the same amplitudes are given.

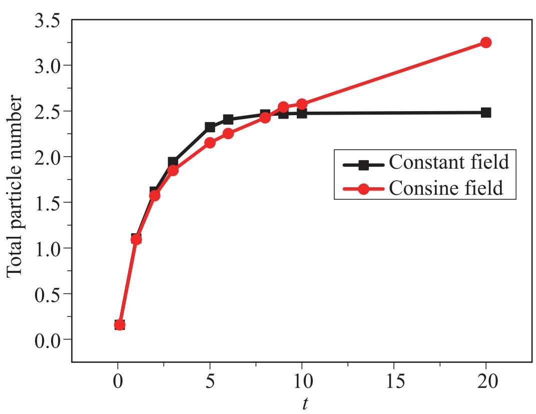

Fig. 5 Total produced particle number on $\boldsymbol{Q}$ sphere for fermions as a function of t.

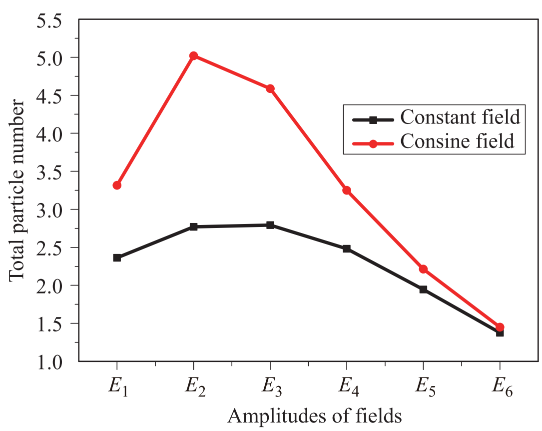

Fig. 6 Total produced particle number on $\boldsymbol{Q}$ sphere for fermions as a function of fields amplitude at $t = 20$. The field amplitudes E_i with $i = 1$ to $i = 6$ are the same as in Fig. 2.

6 Conclusion and discussion

It is interesting that when the distribution of particle production on the $\boldsymbol{Q}$ sphere is calculated, the particle number density is distributed over two islands and moves on the $\boldsymbol{Q}$ sphere as it evolves. The distribution is initially centered, splits into two parts that move to each edge of the islands, and ultimately reaches a steady state. We comprehend this as a preproduction process according to the classical description, which means we can see that non-Abelian production does not occur immediately but in a process over time. Further, we regard the two centrosymmetric islands as the color charge space of conjugated particles. From our calculation, we also find that the steady state that the distribution can reach is related to the amplitude and variation of the field in space-time.

There are two colors in the $SU(2)$ case, and they are related to one Casimir invariant (which could be described by two parameters on a sphere). In our paper, the color charges ($\boldsymbol{Q}$) are included as the Darboux variables. We understand that the non-Abelian interaction occurs as the color charge moves on the $\boldsymbol{Q}$ sphere. Because our calculation is based on a classical model, the color charges vary continuously on the sphere. Further, particle production is related not only to the particle number but also to the splittings, in which the base colors should be well defined.

The other important consideration is the Pauli blocking effect, which is not included in this work. In fact, we made some calculations for this problem that included the Pauli blocking effect and found that a similar preproduction process exists. Certainly the difference in the quantitative results obtained with and without the Pauli blocking effect is worth studying further.

For future work, it is necessary to define the base color properly and find the value of the critical amplitude that leads to splitting. In addition, extending the problem to the $SU(3)$ case and comparing the results with those of quantum field theory are also important and necessary.

Acknowledgements This work was supported by the National Natural Science Foundation of China (NSFC) under Grant No. 11475026. The computation was carried out at the HSCC of the Beijing Normal University.

Appendix A Motion equations

To simplify the formalism, we choose a gauge and require the field $A^{a,\mu}(x)$ in the z direction depending only on t

for all $a = 1, 2, 3$, which reads as

$$A^{a,\mu}(t) = (0, 0, 0, A^a(t)). \tag{A1}$$

We can easily find the nonvanishing field terms when $\mu = z, \nu = t$ or $\mu = t, \nu = z$, which give

$$F^a_{t,z}(t) = -F^a_{z,t}(t) = -\partial_t A^a(t) \equiv E^a(t). \tag{A2}$$

From Eq. (5), the nonvanishing terms are

$$\partial_t F^{a,tz}(t) = -\partial E^a(t) \equiv J^{a,z}(t), \tag{A3}$$
$$g f^{abc} A^b_z t F^{a,zt}(t) = g f^{abc} A^b_z t E^c(t) \equiv J^{a,t}(t). \tag{A4}$$

Writing these equations in vector notation yields

$$\partial_t \boldsymbol{A}(t) = -\boldsymbol{E}(t), \tag{A5}$$
$$\partial_t \boldsymbol{E}(t) = -\boldsymbol{J}^z(t), \tag{A6}$$
$$g\boldsymbol{A}(t) \times \boldsymbol{E}(t) = \boldsymbol{J}^t(t), \tag{A7}$$

and from Eqs. (A5)–(A7), we have

$$\partial_t \boldsymbol{J}^t(t) + g\boldsymbol{A}(t) \times \boldsymbol{J}^z(t) = 0. \tag{A8}$$

Inserting these equations into Eqs. (6)–(8), Wong's equations can be obtained as

$$m\frac{\mathrm{d}t(\tau)}{\mathrm{d}\tau} = p^t(\tau), \tag{A9}$$
$$m\frac{\mathrm{d}z(\tau)}{\mathrm{d}\tau} = p^z(\tau), \tag{A10}$$
$$m\frac{\mathrm{d}p^t(\tau)}{\mathrm{d}\tau} = g\boldsymbol{Q}(\tau) \cdot \boldsymbol{E}(\tau) p^z(\tau), \tag{A11}$$
$$m\frac{\mathrm{d}p^z(\tau)}{\mathrm{d}\tau} = g\boldsymbol{Q}(\tau) \cdot \boldsymbol{E}(\tau) p^t(\tau), \tag{A12}$$
$$m\frac{\mathrm{d}\boldsymbol{Q}(\tau)}{\mathrm{d}\tau} = g\boldsymbol{A}(\tau) \times \boldsymbol{Q}(\tau) p^z(\tau). \tag{A13}$$

By taking a dot product with $\boldsymbol{Q}(\tau)$ in Eq. (A13), we can easily see that Q^2 is a conserved quantity. Further, by taking a dot product with $\boldsymbol{A}(\tau)$ in Eq. (A13), we obtain

$$m\boldsymbol{A}(\tau) \cdot \frac{\mathrm{d}\boldsymbol{Q}(\tau)}{\mathrm{d}\tau} = 0. \tag{A14}$$

Recalling that

$$p^t(\tau)\boldsymbol{E}(\tau) = -m\frac{\mathrm{d}t}{\mathrm{d}\tau}\frac{\boldsymbol{A}(t)}{\mathrm{d}t} = -m\frac{\mathrm{d}\boldsymbol{A}(\tau)}{\mathrm{d}\tau}, \tag{A15}$$

Eq. (A12) can be written as a total derivative,

$$m\frac{\mathrm{d}}{\mathrm{d}\tau}[p^z(\tau) + g\boldsymbol{Q}(\tau) \cdot \boldsymbol{A}(\tau)] = 0 \tag{A16}$$

so that $p^z(\tau) + g\boldsymbol{Q}(\tau) \cdot \boldsymbol{A}(\tau) \equiv P^z$ is a constant of motion.

Appendix B Solution of the B–V equation

We could solve the B–V equation by using the method of characteristics. If we integrate the source over a classical particle path trajectory from τ_0 to τ, and require the field in the z direction and take the p^z distribution only, then the distribution function $f(t, p^z, \boldsymbol{Q})$ reads as

$$f(t, p^z, \boldsymbol{Q}) = f(t(\tau_0), p^z(\tau_0), \boldsymbol{Q}(\tau_0)) + \frac{1}{m}\int_{\tau_0}^{\tau} \mathrm{d}\tau' p^t(\tau')\boldsymbol{C}(t(\tau'), p^z(\tau'), \boldsymbol{Q}(\tau')), \tag{B1}$$

where $t(\tau'), p^z(\tau'), \boldsymbol{Q}(\tau')$ are the solutions of the trajectory equations for values between τ_0 and τ, where the path length is real and $\tau > 0$, which means that the integration is in the light cone as time advances. Because no particles are present at $t = 0$, and thus $f_0(0, p^z(\tau_0), \boldsymbol{Q}(\tau_0))) = 0$, Eq. (B1) becomes

$$f(t, p^z, \boldsymbol{Q}) = \frac{1}{m}\int_{\tau_0}^{\tau} \mathrm{d}\tau' p^t(\tau')\boldsymbol{C}(t(\tau'), p^z(\tau'), \boldsymbol{Q}(\tau')). \tag{B2}$$

Inserting the classical source term, we have

$$f(t, p^z, \boldsymbol{Q}) = \frac{1}{m}\int_{\tau_0}^{\tau} \mathrm{d}\tau' p^t(\tau')|g\boldsymbol{Q}(\tau') \cdot E(\tau')| \times\boldsymbol{R}(\tau', \boldsymbol{Q}(\tau'))\delta(p^z(\tau')); \tag{B3}$$

considering Eqs. (A12) and (B1) and integrating over $p^z(\tau')$, we find

$$f(t(\tau), \boldsymbol{Q}(\tau)) = \sum \boldsymbol{R}(\tau_n, \boldsymbol{Q}(\tau_n))\theta(t(\tau_n))\theta(t - t(\tau_n)), \tag{B4}$$

where τ_n are the solutions of

$$P^z + [\boldsymbol{Q} \cdot \boldsymbol{A} - \boldsymbol{Q}(\tau') \cdot \boldsymbol{A}(\tau')] = 0, \tag{B5}$$

using the relation $\theta(0) = \frac{1}{2}$. Solving Eq. (B4) and defining $f_0(t, 0, \boldsymbol{Q}) \equiv f(t, p^z, \boldsymbol{Q})$ gives

$$f_0(t, \boldsymbol{Q}) = \frac{\boldsymbol{S}(t, \boldsymbol{Q})/2 + \sum_{\tau'_n} \boldsymbol{R}(\tau'_n, \boldsymbol{Q}(\tau)n'))}{1 + \boldsymbol{S}(t, Q)}, \tag{B6}$$

which completes the solution of $f(t, p, \boldsymbol{Q})$ using the method of characteristics. In the special case, once the trajectory equations are solved, the special distribution function can easily be calculated. By substituting the results into Eqs. (9)–(11), the needed current energy, pressures, and number density are obtained:

$$J^z(t) = \int \mathrm{d}\boldsymbol{P}\mathrm{d}\boldsymbol{Q} p^z Q f_0(t, \boldsymbol{Q}), \tag{B7}$$

$$J^t(t) = \int \mathrm{d}\boldsymbol{P}\mathrm{d}\boldsymbol{Q} p^t Q f_0(t, \boldsymbol{Q}), \tag{B8}$$

$$e(t) = \int \mathrm{d}\boldsymbol{P}\mathrm{d}\boldsymbol{Q} {p^t}^2 f_0(t, \boldsymbol{Q}), \tag{B9}$$

$$p^z(t) = \int \mathrm{d}\boldsymbol{P}\mathrm{d}\boldsymbol{Q} p^t p^z f_0(t, \boldsymbol{Q}), \tag{B10}$$

$$n(t) = \int \mathrm{d}\boldsymbol{P}\mathrm{d}\boldsymbol{Q} f_0(t, \boldsymbol{Q}). \tag{B11}$$

References

1. U. Heinz, Kinetic theory for plasmas with non-Abelian interactions, *Phys. Rev. Lett.* 51(5), 351 (1983)
2. U. Heinz, The approach to equilibrium in a quark-gluon plasma, *Z. Phys. C* 38(1–2), 203 (1988)
3. U. Heinz, Non-equilibrium dynamics in finite-temperature QCD, *Physica A* 158(1), 111 (1989)
4. P. F. Kelly, Q. Liu, C. Lucchesi, and C. Manuel, Deriving the hard thermal loops of QCD from classical transport theory, *Phys. Rev. Lett.* 72(22), 3461 (1994)
5. P. F. Kelly, Q. Liu, C. Lucchesi, and C. Manuel, Classical transport theory and hard thermal loops in the quark-gluon plasma, *Phys. Rev. D* 50(6), 4209 (1994)
6. D. Bödeker, Effective dynamics of soft non-Abelian gauge fields at finite temperature, *Phys. Lett. B* 426(3–4), 351 (1998)
7. D. Bödeker, From hard thermal loops to Langevin dynamics, *Nucl. Phys. B* 559(1–2), 502 (1999)
8. D. Bödeker, Diagrammatic approach to soft non-Abelian dynamics at high temperature, *Nucl. Phys. B* 566(1–2), 402 (2000)
9. D. F. Litim and C. Manuel, Semi-classical transport theory for non-Abelian plasmas, *Phys. Rep.* 364(6), 451 (2002)
10. J. Shwinger, On gauge invariance and vacuum polarization, *Phys. Rev.* 82(5), 664 (1951)
11. J. F. Dawson, B. Mihaila, and F. Cooper, Fermion particle production in semiclassical Boltzmann-Vlasov transport theory, *Phys. Rev. D* 80(1), 014011 (2009)
12. B. Mihaila, F. Cooper, and J. F. Dawson, Backreaction and particle production in (3+1)-dimensional QED, *Phys. Rev. D* 80(1), 014010 (2009)
13. N. Abdukerim, Z. L. Li, and B. S. Xie, Effects of laser pulse shape and carrier envelope phase on pair production, *Phys. Lett. B* 726(4–5), 820 (2013)
14. N. Abdukerim, Z. L. Li, and B. S. Xie, Electron-positron pair production in the low-density approximation, *Front. Phys.* 10(4), 101202 (2015)
15. Z. L. Li, D. Lu, and B. S. Xie, Dynamically assisted pair production for scalar QED by two fields, *Front. Phys.* 10, 101201 (2015)
16. O. Oluk, B. S. Xie, M. A. Bake, and S. Dulat, Electron-positron pair production in a strong asymmetric laser electric field, *Front. Phys.* 9(2), 157 (2014)
17. Z. L. Li, D. Lu, B. S. Xie, L. B. Fu, J. Liu, and B. F. Shen, Enhanced pair production in strong fields by multiple-slit interference effect with dynamically assisted Schwinger mechanism, *Phys. Rev. D* 89(9), 093011 (2014)
18. Z. L. Li, D. Lu, B. S. Xie, B. F. Shen, L. B. Fu, and J. Liu, Nonperturbative signatures in pair production for general elliptic polarization fields, *Europhys. Lett.* 110(5), 51001 (2015)
19. Z. L. Li, D. Lu, and B. S. Xie, Effects of electric field polarizations on pair production, *Phys. Rev. D* 92(8), 085001 (2015)
20. G. C. Nayak and P. van Nieuwenhuizen, Soft-gluon production due to a gluon loop in a constant chromoelectric background field, *Phys. Rev. D* 71(12), 125001 (2005)
21. G. C. Nayak, Nonperturbative quark-antiquark production from a constant chromoelectric field via the Schwinger mechanism, *Phys. Rev. D* 72(12), 125010 (2005)
22. J. F. Dawson, B. Mihaila, and F. Cooper, Dynamics of particle production by strong electric fields in non-Abelian plasmas, *Phys. Rev. D* 81(5), 054026 (2010)
23. F. Cooper, J. F. Dawson, and B. Mihaila, Casimir dependence of transverse distribution of pairs produced from a strong constant chromoelectric background field, *Phys. Rev. D* 78(11), 117901 (2008)
24. V. V. Skokov and P. Lévai, Transverse and longitudinal momentum spectra of fermions produced in strong $SU(2)$ fields, *Phys. Rev. D* 78(5), 054004 (2008)
25. S. K. Wong, Field and particle equations for the classical Yang-Mills field and particles with isotopic spin, *Nuvo. Cimemto. A.* 65(4), 689 (1970)
26. H. Kleinert, R. Ruffini, and S. S. Xue, Electron-positron pair production in space- or time-dependent electric fields, *Phys. Rev. D* 78(2), 025011 (2008)